# GRAPH REPRESENTATION LEARNING FOR SPATIAL IMAGE STEGANALYSIS

*Qiyun Liu and Hanzhou Wu*

Shanghai University, Shanghai 200444, China

## ABSTRACT

In this paper, we introduce a graph representation learning architecture for spatial image steganalysis, which is motivated by the assumption that steganographic modifications unavoidably distort the statistical characteristics of the hidden graph features derived from cover images. In the detailed architecture, we translate each image to a graph, where nodes represent the patches of the image and edges indicate the local associations between the patches. Each node is associated with a feature vector determined from the corresponding patch by a shallow convolutional neural network (CNN) structure. By feeding the graph to an attention network, the discriminative features can be learned for efficient steganalysis. Experiments indicate that the reported architecture achieves a competitive performance compared to the benchmark CNN model, which has shown the potential of graph learning for steganalysis.

***Index Terms***— Steganalysis, graph neural networks, attention mechanism, deep learning.

## 1. INTRODUCTION

Steganographic traces can be well concealed by the intrinsic noise-like components of the cover image, which are often located in the high-frequency regions. It inspires us to preferentially embed secret data into these hard-to-notice regions with an adaptive mechanism [1], or the minimal-distortion framework [2], to better resist against steganalysis. Many works are designed along this line such as [3, 4, 5]. Unlike the above-mentioned algorithms that follow the paradigm of minimizing the total embedding cost, another principle for steganographic design is to preserve the chosen model of the cover, which is provably secure with respect to the chosen model such as [6]. Recent works bring closer the relationship between cost based steganography and model based steganography [7].

As the opposite to steganography, (image) steganalysis is to determine whether a given image contains hidden information or not. It can be divided into *targeted steganalysis* and *blind steganalysis*. While the former uses the prior knowledge about the specific steganographic algorithm to identify stegos created by the steganographic algorithm, the latter aims to determine whether a given media contains secret information or not without any side information about the steganographic algorithm. Targeted steganalysis usually shows the better detection performance than blind steganalysis since steganographic traces are more likely to be reliably captured given the embedding mechanism of the steganographic algorithm. However, in applications, blind steganalysis is more desirable than targeted steganalysis since it is often the case that the used steganographic algorithm is unknown to us, resulting in that the majority of steganalysis works are (semi-)blind systems.

From the perspective of design principle, early steganalysis extracts manually-crafted features from media objects and then uses conventional statistical analysis tools such as support vector machine and linear discriminant analysis for classification. E.g., Markov-based features have been widely used in early image steganalysis such as [8, 9, 10]. Though *ensemble* and *dimensionality reduction* can be utilized to enhance the detection performance [11], these algorithms rely heavily on sophisticated manual feature design and become hard to improve due to the advancement of steganography that tends to alter pixels in image regions that are hard to detect. In order to overcome this difficulty, in recent years, in-depth studies are performed on moving the success achieved by deep convolutional neural networks (deep CNNs) [12] in computer vision to image steganalysis [13, 14, 15, 16, 17, 18]. These works can be briefly generalized by three phases, i.e., *residual determination*, *feature learning* and *binary classification*. Specifically, they first filter the input image to generate residual image(s). It enlarges the signal-to-noise ratio between the noise-like stego signal and the host signal and therefore facilitates the feature learning procedure. By providing the residual image(s) to the deep CNN architecture, discriminative features can be learned and utilized for binary classification. The entire process can be implemented by an end-to-end fashion.

Recently, there is increasing interest in extending the deep learning paradigms to graph data, promoting graph neural network (GNN) to become a hot topic [19]. GNNs are essentially graph representation learning models and can be well applied to node-focused tasks and graph-focused tasks. By modelling digital images as graph data structures, many visual problems can be effectively solved with GNNs. Motivated by this point, despite the superiority of CNNs in image steganalysis, in this paper, we make the step towards GNN based image steganaly-
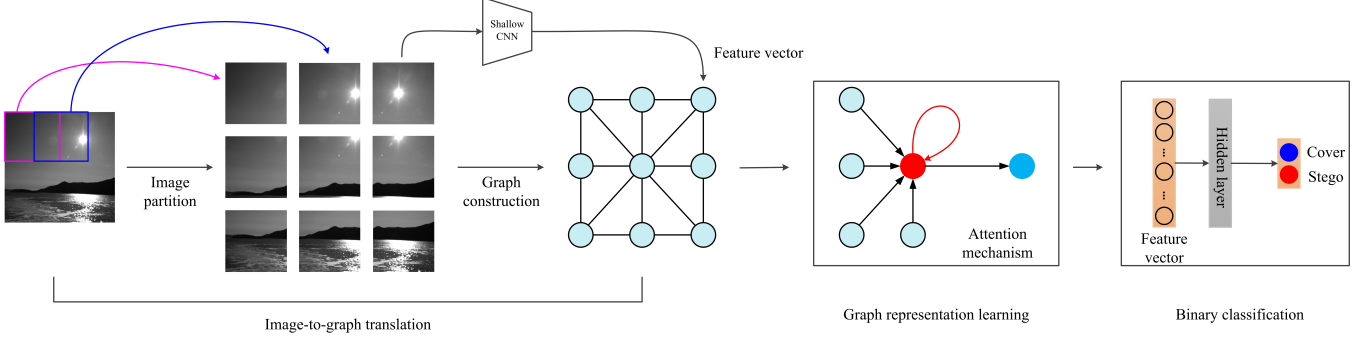
**Fig. 1**. Sketch for the proposed GNN based architecture for spatial image steganalysis.

sis. Our experimental results indicate that the proposed GNN based architecture achieves a competitive performance, which shows the potential of graph representation learning for image steganalysis and can inspire follow-up works.

The rest of this paper will be organized as follows. In Section 2, we detail the proposed work, followed by experimental results in Section 3. We conclude this paper in Section 4.

## 2. PROPOSED METHOD

As shown in Fig. 1, the proposed architecture consists of three phases, i.e., *image-to-graph translation*, *graph representation learning* and *binary classification*. The purpose of image-to-graph translation is to convert an image to a graph with feature vectors assigned to the nodes. The graph can be then fed to a graph attention network for representation learning, allowing the outputted feature vector to be used for final classification. We show more technical details in the following subsections.

### 2.1. Image-to-Graph Translation

Given a gray-scale image $\mathbf{I} = \{x_{i,j} | 1 \le i \le h, 1 \le j \le w\}$, where $x_{i,j} \in \{0, 1, ..., 255\}$, we first partition $\mathbf{I}$ into $n \times m$ patches, where $n \le h, m \le w$. A patch is defined as a sub-image of $\mathbf{I}$ with a size of $h_p \times w_p$, where $h_p \le h$ and $w_p \le w$. Let $\{\mathbf{I}_{u,v} | 1 \le u \le n, 1 \le v \le m\}$ represent the patches obtained by raster scan, where $\mathbf{I}_{u,v}$ means the patch located at position $(u, v)$, e.g., for the $3 \times 3$ patches shown in Fig. 1, the central patch has a position index of $(2, 2)$. The first step of image-to-graph translation is to compute all $\mathbf{I}_{u,v}$ defined as:

$$\mathbf{I}_{u,v} = \{x_{i,j} | i \in [f_{u,v}, f_{u,v} + h_p), j \in [g_{u,v}, g_{u,v} + w_p)\},$$

where $(f_{u,v}, g_{u,v})$ represents the position in $\mathbf{I}$ for the top-left pixel of $\mathbf{I}_{u,v}$. Initially, we have $f_{1,1} = g_{1,1} = 1$ and

$$f_{u,v} = f_{u,v-1}, g_{u,v} = g_{u-1,v}, \forall u \in [2, n], v \in [2, m]. \quad (1)$$

For $v \in [2, m]$, $g_{u,v}$ is determined by:

$$g_{u,v} = g_{u,v-1} + (1 - \alpha) \cdot w, \quad (2)$$

where $\alpha \in [0, 1)$ is the parameter used to control the area of intersection between $\mathbf{I}_{u,v}$ and $\mathbf{I}_{u,v-1}$, e.g., $\alpha = 0.3$ means 30% pixels in $\mathbf{I}_{u,v}$ are also belonging to $\mathbf{I}_{u,v-1}$. Similarly, for $2 \le u \le n$, $f_{u,v}$ is determined by:

$$f_{u,1} = f_{u-1,1} + (1 - \beta) \cdot h, \quad (3)$$

where $\beta$ controls the area of intersection between $\mathbf{I}_{u-1,1}$ and $\mathbf{I}_{u,1}$. By default, we use $\alpha = \beta$ unless otherwise specified.

For example, assuming that $h = w = 2h_p = 2w_p = 512$, we have 4 disjoint patches if $\alpha = 0$ and $n = m = 2$. And, $(f_{1,1}, g_{1,1}) = (1, 1)$, $(f_{1,2}, g_{1,2}) = (1, 257)$, $(f_{2,1}, g_{2,1}) = (257, 1)$, $(f_{2,2}, g_{2,2}) = (257, 257)$. We have 9 patches if $\alpha = 0.5$ and $n = m = 3$. Moreover, the top-left pixel-positions are $(1, 1)$, $(1, 129)$, $(1, 257)$, $(129, 1)$, $(129, 129)$, $(129, 257)$, $(257, 1)$, $(257, 129)$ and $(257, 257)$, respectively.

In order to construct a graph, each patch will be mapped to a graph node. Then, edges should be assigned to node-pairs. It is open for us to design the edge insertion mechanism. For example, for any two different nodes, we add an edge between them so that a *complete graph* is generated. We can also use the spatial relationship between nodes to construct the graph. For example, for two patches $\mathbf{I}_{a,b}$ and $\mathbf{I}_{c,d}$, we add an edge between the corresponding two nodes if $\max(|a-b|, |c-d|) = 1$. We define such kind of graph as a *lattice graph*.

The graph nodes should be associated with feature vectors beneficial to steganalysis. To this end, we use a shallow CNN to reduce each high-dimensional patch to a low-dimensional feature vector that will be assigned to the corresponding node. It is open for us to design the CNN. For simplicity, we use our previously designed XWS-CNN (co-authored with G. Xu and Y. Shi) [14] for feature extraction. The XWS-CNN has a high-pass filtering layer, five conv-pooling layers and a linear classification layer. For feature extraction, we only use the high-pass filtering layer and the conv-pooling layers, enabling each patch to be mapped to a $l$-D feature vector, where $l$ is tunable, e.g., $l = 128$ for raw XWS-CNN reported in [14].

Though XWS-CNN itself has demonstrated superior performance in image steganalysis, we are to show in our experiments that the steganalysis performance of XWS-CNN will decline significantly by reducing the number of conv-pooling

layers. However, by applying the graph representation learning strategy after reducing the conv-pooling layers, the image steganalysis performance can be well maintained, indicating that graph learning plays an important role in steganalysis.

All patches will be processed with the same CNN. In other words, only one CNN module is trained, which has a lower computational cost and reduces the mismatch impact between multiple CNNs and multiple patches caused by diversity.

## 2.2. Graph Representation Learning

The image-to-graph translation procedure enables us to construct a graph containing $nm$ nodes, which can be expressed as two matrices $\mathbf{A} \in \{0,1\}^{nm \times nm}$ and $\mathbf{W} \in \mathbb{R}^{nm \times l}$. Here, $\mathbf{A}$ means the adjacency matrix and $\mathbf{W}$ denotes the node features in the matrix form. The purpose of graph representation learning is to use a GNN to generate a representation (embedding) for each node in the above graph so that the node embeddings in the matrix form can be used to determine whether the corresponding image is *stego* or not. We have evaluated various GNNs and finally decided to use the graph attention network (GAT) [20] due to its superiority for steganalysis. Following the neighborhood aggregation paradigm, GAT takes as input a graph (including its topological structure and descriptive features) and produces a representation for each graph node. The representation for each node can be expressed as a vector. We refer the reader to [20] for more details. One thing to note is that before feeding $\mathbf{A}$ to the GAT, for each node, we add an edge to connect the node itself, i.e., $a_{i,i} = 1$ for all $a_{i,i} \in \mathbf{A}$. In addition, *multi-head attention* [20] is not used in this paper.

## 2.3. Binary Classification

To achieve graph-level classification, a *readout* function [19] is used to generate a representation (embedding) of the entire graph according to the final node representations of GAT. In other words, the readout operation maps the final node representations in the matrix form to a real vector. The graph-level representation will be thereafter fed to a 64-D fully-connected hidden layer equipped with ReLU [21], and then processed by a 2-D classification layer with softmax to output probabilities.

## 3. EXPERIMENTAL RESULTS AND ANALYSIS

### 3.1. Basic Setup

The steganographic algorithms tested in experiments included S-UNIWARD [5] and HILL [4]. The popular BOSSBase 1.01 [3] dataset containing 10,000 natural images sized $512 \times 512$ was used for generating stego images. For each experiment, out of 10,000 pairs of (cover/stego) images, 4,000 pairs were used for model training, 1,000 pairs were used for model validation and the rest 5,000 pairs were used for model testing. The three subsets did not intersect with each other.
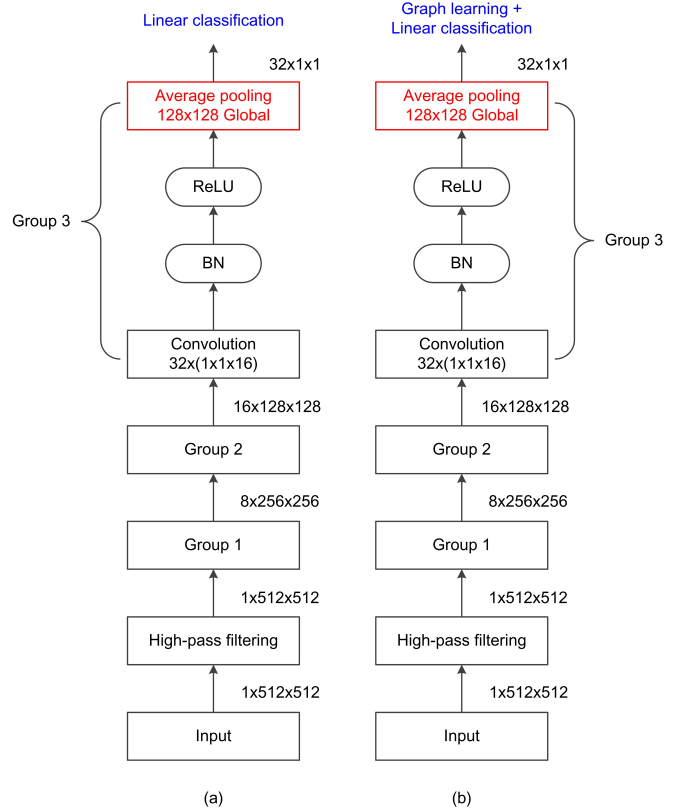


**Fig. 2**. An example of the shallow CNN: (a) CNN-G3-32 and (b) CNN-GAT-G3-32. The input size $512 \times 512$ is adjustable, e.g., it should be $256 \times 256$ when we have $h_p = w_p = 256$.
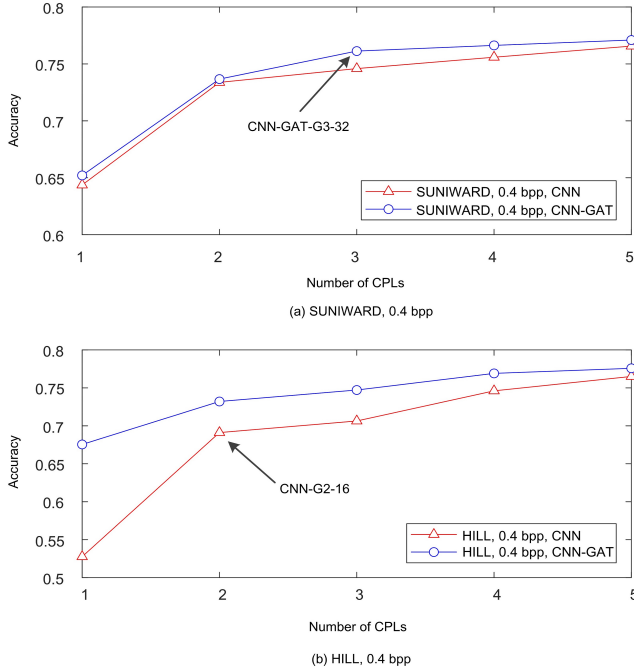
We used PyTorch for simulation, accelerated with a single TITAN RTX 24 GB GPU. The batch size was set to 32, and the total number of epochs was set to 300, leading to a total of 75,000 (= $8000/32 \times 300$) iterations for training a model. The learning rate was set to 0.001 and the Adam optimizer [22] (with two hyper-parameters $\beta_1 = 0.5, \beta_2 = 0.999$) was used to update model parameters, which were initialized with the default settings provided by PyTorch.

Our GAT implementation based on the open source code[1]. In experiments, the number of graph attention layers (GALs) was set to 2. The readout function used the "average" operation to fuse the node representations. The dimension of the final graph-level representation processed with readout equals that of the representation of each graph node. We used *complete graph* for training in order that the model fully exploits the associations between any two patches. In addition, each patch has a size of $256 \times 256$. $n = m = 3$ and $\alpha = \beta = 0.5$.

### 3.2. Shallow CNN

As mentioned previously, we use the high-pass filtering (HPF) layer and conv-pooling layers (CPLs) of XWS-CNN [14] to
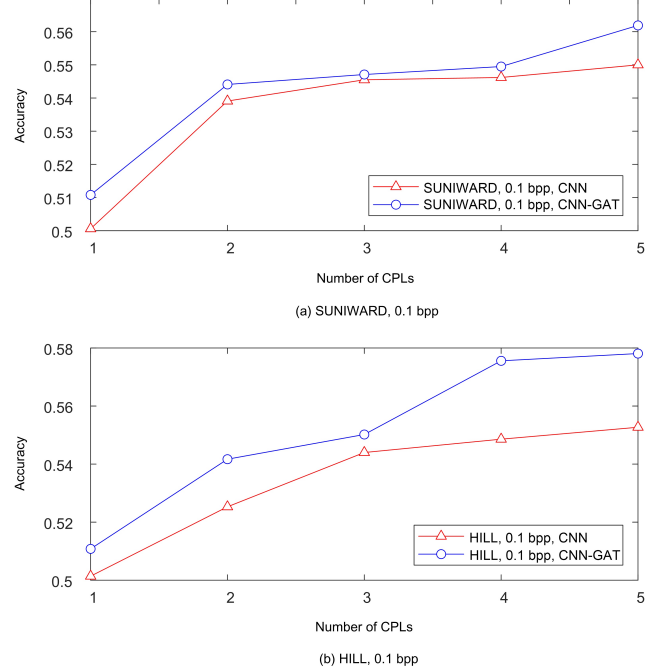
---

[1]https://github.com/Diego999/pyGAT

**Fig. 3**. Detection accuracy with an embedding rate of 0.4 bpp.



**Fig. 4**. Detection accuracy with an embedding rate of 0.1 bpp.

constitute the shallow CNN. There are 5 CPLs in XWS-CNN. By orderly collecting the CPLs, we can construct 5 shallow CNNs. For example, the shallow CNN may only consist of the HPF layer and Group 1 of XWS-CNN. To guarantee that the feature vector outputted by each shallow CNN can be directly fed to the linear classification layer or the graph learning layer, the average pooling operation was set to *global*. Fig. 2 shows an example of the shallow CNN using the first three groups of XWS-CNN, based on which it is straightforward to construct the other shallow CNNs. Obviously, the 5 shallow CNNs can be directly used for classification by adding a linear classification layer. We term them as CNN-G1-8, CNN-G2-16, CNN-G3-32, CNN-G4-64 and CNN-G5-128, respectively, e.g., "CNN-G5-128" means to use 5 groups to produce a 128-D feature vector for binary classification, which is exactly XWS-CNN. By adding the graph learning and classification module, we can also build 5 models for steganalysis. We term them as CNN-GAT-G1-8, CNN-GAT-G2-16, CNN-GAT-G3-32, CNN-GAT-G4-64 and CNN-GAT-G5-128.

### 3.3. Results

The detection accuracy, which is defined as the percentage of correctly classified images, was used to evaluate the steganalysis performance. Following mainstream works, we took into account two representative embedding rates, i.e., 0.4 bpp (bits per pixel) and 0.1 bpp. Fig. 3 and Fig. 4 show the steganalysis results with an embedding rate of 0.4 bpp and 0.1 bpp respectively for S-UNIWARD and HILL using different neural networks. From the two figures, we conclude that: First,

the proposed graph learning architecture significantly outperforms the benchmark CNN model in terms of detection accuracy, which shows the superiority of graph learning for steganalysis. Second, comparing with the CNN model, the performance degradation rate of graph learning is lower. In other words, by reducing the number of CPLs, the proposed work can still achieve a relatively higher accuracy, e.g., for HILL with an embedding rate of 0.4 bpp shown in Fig. 3, the detection accuracy is 0.7321 when the number of CPLs is 2 and 0.6755 when the number of CPLs is only 1, which are significantly higher than that for the CNN model, which implies that graph learning has the ability to well exploit statistical features and structural information for efficient steganalysis.

## 4. CONCLUSION

We present a general graph learning framework for spatial image steganalysis, which can be easily extended to other cover sources. Experiments show that the proposed work outperforms the benchmark CNN model, which has verified the superiority and applicability of graph representation learning for steganalysis. Obviously, one may use ensemble, prior knowledge (e.g., probability maps of embedding), hyper-parameter tuning techniques and other tricks to enhance the steganalysis performance. Our original intention was not to increase the accuracy by a few percentages. Instead, the main contribution of this paper is to reveal that graph learning has the potential to achieve the state-of-the-art performance in steganalysis. In future, we will exploit graph learning for JPEG steganalysis.

# 5. REFERENCES

[1] W. Luo, F. Huang, and J. Huang, "Edge adaptive image steganography based on LSB matching revisited," *IEEE Trans. Inf. Forensics Security*, vol. 5, no. 2, pp. 201-214, 2010.

[2] T. Filler, J. Judas, and J. Fridrich, "Minimizing additive distortion in steganography using syndrome-trellis codes," *IEEE Trans. Inf. Forensics Security*, vol. 6, no. 3, pp. 920-935, 2011.

[3] T. Pevny, T. Filler, and P. Bas, "Using high-dimensional image models to perform highly undetectable steganography," In: *Proc. Int. Workshop Inf. Hiding*, pp. 161-177, 2020.

[4] B. Li, M. Wang, J. Huang, and X. Li, "A new cost function for spatial image steganography," In: *IEEE Int. Conf. Image Process.*, pp. 4206-4210, 2014.

[5] V. Hulub, J. Fridrich, and T. Denemark, "Universal distortion function for steganography in an arbitrary domain," *EURASIP J. Inf. Security*, vol. 2014, no. 1, pp. 1-13, 2014.

[6] K. Solanki, K. Sullivan, U. Madhow, B. S. Manjunath, and S. Chandrasekaran, "Provably secure steganography: achieving zero K-L divergence using statistical restoration," In: *Proc. IEEE Int. Conf. Image Process.*, pp. 125-128, 2006.

[7] J. Butora, Y. Yousfi, and J. Fridrich, "Turning cost-based steganography into model-based," In: *Proc. ACM Workshop Inf. Hiding Multimed. Security*, pp. 151-159, 2020.

[8] Y. Shi, C. Chen, and W. Chen, "A Markov process based approach to effective attacking JPEG steganography," In: *Proc. Int. Workshop Inf. Hiding*, pp. 249-264, 2006.

[9] T. Pevny, P. Bas, and J. Fridrich, "Steganalysis by subtractive pixel adjacency matrix," *IEEE Trans. Inf. Forensics Security*, vol. 5, no. 2, pp. 215-224, 2010.

[10] J. Fridrich, and J. Kodovsky, "Rich models for steganalysis of digital images," *IEEE Trans. Inf. Forensics Security*, vol. 7, no. 3, pp. 868-882, 2012.

[11] H. Wu, "Unsupervised steganographer identification via clustering and outlier detection," In: *Digital Media Steganography*, Academic Press, pp. 295-319, 2020.

[12] A. Krizhevsky, I. Sutskever, and G. E. Hinton, "ImageNet classification with deep convolutional neural networks," In: *Proc. Neural Inf. Process. Syst.*, pp. 1097-1105, 2012.

[13] Y. Qian, J. Dong, W. Wang, and T. Tan, "Deep learning for steganalysis via convolutional neural networks," In: *Proc. IS&T Electronic Imaging, Media Watermarking, Security, and Forensics*, pp. 171-180, 2015.

[14] G. Xu, H. Wu, and Y. Shi, "Structural design of convolutional neural networks for steganalysis," *IEEE Signal Process. Lett.*, vol. 5, no. 23, pp. 708-712, 2016.

[15] G. Xu, H. Wu, and Y. Shi, "Ensemble of CNNs for steganalysis: an empirical study," In: *Proc. ACM Workshop Inf. Hiding Multimed. Security*, pp. 103-107, 2016.

[16] M. Boroumand, M. Chen, and J. Fridrich, "Deep residual network for steganalysis of digital images," *IEEE Trans. Inf. Forensics Security*, vol. 14, no. 5, pp. 1181-1193, 2018.

[17] J. Ye, J. Ni, and Y. Yi, "Deep learning hierarchical representations for image steganalysis," *IEEE Trans. Inf. Forensics Security*, vol. 12, no. 11, pp. 2545-2557, 2017.

[18] S. Wu, S. Zhong, and Y. Liu, "Deep residual learning for image steganalysis," *Multimed. Tools Appl.*, vol. 77, no. 9, pp. 10437-10453, 2018.

[19] Z. Wu, S. Pan, F. Chen, G. Long, C. Zhang, and P. S. Yu, "A comprehensive survey on graph neural networks," *arXiv preprint arXiv:1901.00596*, 2019.

[20] P. Velickovic, G. Cucurull, A. Casanova, A. Romero, P. Lio, and Y. Bengio, "Graph attention networks," *arXiv preprint arXiv:1710.10903*, 2017.

[21] B. Xu, N. Wang, T. Chen and M. Li, "Empirical evaluation of rectified activations in convolutional network," *arXiv preprint arXiv:1505.00853*, 2015.

[22] D. P. Kingma and J. Ba, "Adam: a method for stochastic optimization," *arXiv:1412.6980*, 2014.